

The Enhancement Role of ZnO Surface Modification on Electrochemical Performance of $\text{Li}_4\text{Ti}_5\text{O}_{12}/\text{ZnO}$ Composites

Ting Zhou¹, Yingbin Lin^{1,*}, Guiying Zhao¹, Yandan Huang¹, Heng Lai¹, Jiaxin Li¹, Zhigao Huang^{1,**}, She-huang Wu²

¹ College of Physics and Energy, Fujian Normal University, Fuzhou 350007, China

² Department of Materials Engineering, Tatung University, 40, Changshan N. Rd., Sec. 3, Taipei 104, Taiwan

*E-mail: yblin@fjnu.edu.cn; zg Huang@fjnu.edu.cn

Received: 24 November 2012 / Accepted: 15 December 2012 / Published: 1 January 2013

$\text{Li}_4\text{Ti}_5\text{O}_{12}/\text{ZnO}$ composites have been synthesized as anode material for lithium ion batteries by a mechanical method and the effect of high electronic-conductive ZnO incorporation on the electrochemical performances of $\text{Li}_4\text{Ti}_5\text{O}_{12}$ is investigated systematically by charge/discharge testing, cyclic voltammograms and AC impedance spectroscopy, respectively. In comparison with the pristine $\text{Li}_4\text{Ti}_5\text{O}_{12}$, $\text{Li}_4\text{Ti}_5\text{O}_{12}/\text{ZnO}$ demonstrates superior electrochemical performance in wide operation temperatures, especially at high discharging rates. The analysis of the electrical properties and electrochemical measurements reveal that $\text{Li}_4\text{Ti}_5\text{O}_{12}/\text{ZnO}$ has much lower charge-transfer resistances and higher lithium diffusion rate, especially at low temperature.

Keywords: Lithium-ion batteries; Lithium titanate; Zinc Oxide; High-rate capability; Photoluminescence.

1. INTRODUCTION

In recent years, an increasing attention has been paid to lithium ion batteries due to their potential applications in the field of hybrid electric vehicles (HEVs), plug-in hybrid electric vehicles and electrical energy systems [1-3]. Spinel $\text{Li}_4\text{Ti}_5\text{O}_{12}$ is considered as an alternative anode material to carbon-based materials because of its high structural stability during the discharge/charge processes and relatively high lithium insertion/extraction potential at approximately 1.55 V [4-6]. However, the intrinsic low lithium-ion conductivity and electronic conductivity of bulk $\text{Li}_4\text{Ti}_5\text{O}_{12}$ have been major obstacles to electrochemical extraction of lithium, which causes a steep falling in capacity at high rates [7, 8]. To improve the high rate performance of spinel $\text{Li}_4\text{Ti}_5\text{O}_{12}$, Tremendous efforts have been devoted and the surface coating with high conductive material is proved to be a promising way, such

as carbon and Ag [9-11]. For instance, Guo et al. [9] found that the surface modified $\text{Li}_4\text{Ti}_5\text{O}_{12}$ with carbon exhibits high discharge capacity of 137 mAhg^{-1} at 20 C and remains 125 mAhg^{-1} after 100 cycles. Liu et al. [10] reported that the surface modified $\text{Li}_4\text{Ti}_5\text{O}_{12}$ by Ag nanoparticles displays an excellent high-rate capacity of 131 mAhg^{-1} at 30 C, retaining over 98% after 120 cycles. ZnO with enriching oxygen vacancies seems to be a promising alternative surface modification material for improving rate capability due to its high electronic conductivity, facile fabrication and low cost. In addition, ZnO is a promising anode material with high theoretical capacity of 978 mAhg^{-1} [12, 13]. Combining the above ideas, composing $\text{Li}_4\text{Ti}_5\text{O}_{12}$ with high electronic conductive ZnO would be reasonably beneficial for improving the rate capability and cyclic reversibility of $\text{Li}_4\text{Ti}_5\text{O}_{12}$. In present work, $\text{Li}_4\text{Ti}_5\text{O}_{12}/\text{ZnO}$ is prepared by a simple ball-milling with incorporation of high electronic conductive ZnO nanoparticles. In comparison with the pristine $\text{Li}_4\text{Ti}_5\text{O}_{12}$, the as-prepared $\text{Li}_4\text{Ti}_5\text{O}_{12}/\text{ZnO}$ demonstrates superior electrochemical performances in a wide temperature range, especially at high C-rate.

2. EXPERIMENTAL

2.1. Materials synthesis

$\text{Li}_4\text{Ti}_5\text{O}_{12}$ (lithium titanate) was prepared by a simple solid-state reaction method using commercial TiO_2 as the titanium source with 3wt% LiOH excess stoichiometry to compensate for lithia volatilization during the high-temperature calcination. After planetary-milled in ethanol for 24 h and subsequently dried at 80°C in air, the resulted precursor was calcined at 850°C for 16 h to obtain spinel $\text{Li}_4\text{Ti}_5\text{O}_{12}$ powders. $(\text{Li}_4\text{Ti}_5\text{O}_{12})_{100}/(\text{ZnO})_6$ composite was prepared by mixing $\text{Li}_4\text{Ti}_5\text{O}_{12}$ and commercial ZnO nanoparticles ($\sim 50 \text{ nm}$) through a simple ball-milling approach. In detail, the as-prepared $\text{Li}_4\text{Ti}_5\text{O}_{12}$ powder was ultrasonically dispersed in absolute ethanol containing an appropriate amount of high electronic conductive ZnO nanoparticles. After sonication for 5 h, the reactant precursors were kept ball-milling in ethanol for 20 h and subsequently dried at 110°C in vacuum for 48 h to get the final product.

The phase identification of the pristine $\text{Li}_4\text{Ti}_5\text{O}_{12}$ and $(\text{Li}_4\text{Ti}_5\text{O}_{12})_{100}/(\text{ZnO})_6$ powders was conducted with an X-ray diffractometer (XRD, Rigaku MiniFlex II) using CuK_α radiation ($\lambda=0.15405 \text{ nm}$). The morphology of the composite powder was studied with a scanning electron microscopy (SEM, JSM-7500F, Japan).

2.2 Cell fabrication and characterization

The electrochemical performances of the as-prepared $\text{Li}_4\text{Ti}_5\text{O}_{12}$ and $(\text{Li}_4\text{Ti}_5\text{O}_{12})_{100}/(\text{ZnO})_6$ composite were carried out with coin-type cells (R2025) using metallic lithium film as the counter and reference electrode. The working electrode was prepared by homogeneously pasting a slurry containing 70 wt.% active material, 20 wt.% super-P and 10 wt.% polyvinylidene fluoride (PVDF) dissolved in N-methyl-2-pyrrolidone on copper foil homogeneously and dried in vacuum at 110°C for

12 h. The cells based on the configuration of Li metal(-) | electrolyte | active material(+) were assembled in an argon-filled glove box with Celgard 2300 microporous polyethylene membrane as separator and 1M LiPF₆ in a mixture of ethyl carbonate (EC) and dimethyl carbonate (DMC) (1:1 in vol. ratio) as electrolyte. Charge-discharge performance was characterized galvanostatically on CT2001A cell test instrument (LAND Electronic Co.). Cyclic voltammograms (CV) and electrochemical impedance spectra (EIS) measurements were performed by Arbin 2000 testing system and electrochemical workstation (CHI660C) respectively. The EIS analysis was recorded within frequency ranged between 10 mHz to 100 KHz with an voltage amplitude of 5mV. Electrical properties were measured by a Versalab magnetometer (Versalab free, Quantum Design Co.).

3. RESULTS AND DISCUSSION

3.1 Material Characterization

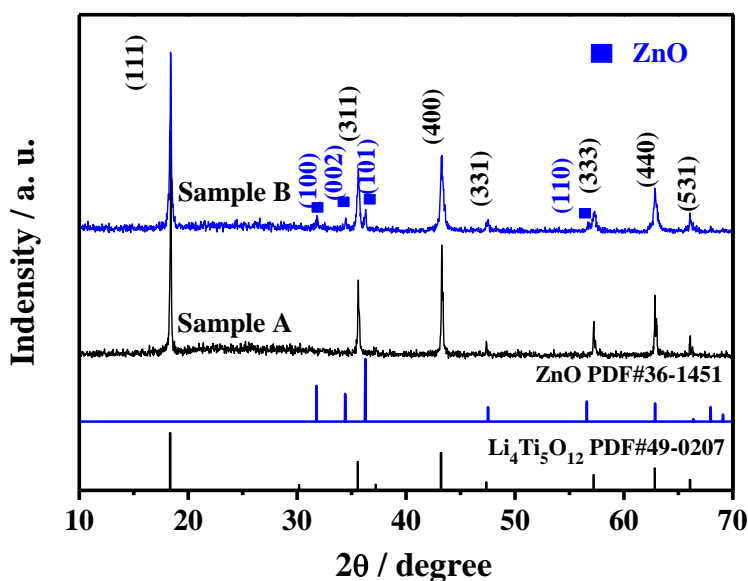


Figure 1. XRD patterns of Sample A and B.

Fig.1 presents XRD patterns of the pristine and $(\text{Li}_4\text{Ti}_5\text{O}_{12})_{100}/(\text{ZnO})_6$ powders, denoted as Samples A and B, respectively. All the observed diffraction peaks for pristine powder can be indexed well based on a $\text{Li}_4\text{Ti}_5\text{O}_{12}$ spinel phase with space group of $Fd3m$ (PDF#49-0207). The diffraction pattern of $(\text{Li}_4\text{Ti}_5\text{O}_{12})_{100}/(\text{ZnO})_6$ is similar to those of the pristine sample, even though nano-sized ZnO particles on the surface. Besides the main $\text{Li}_4\text{Ti}_5\text{O}_{12}$ spinel phase, additional diffraction peaks are also observed, which corresponds to the reflections of wurtzite ZnO (PDF#36-1451).

Figs. 2(a) and (b) show the surface morphologies characterized by SEM for the pristine and $(\text{Li}_4\text{Ti}_5\text{O}_{12})_{100}/(\text{ZnO})_6$ composites, respectively. In comparison with the pristine $\text{Li}_4\text{Ti}_5\text{O}_{12}$, nano-sized ZnO particles are uniformly dispersed on the $\text{Li}_4\text{Ti}_5\text{O}_{12}$ surface. Such ZnO-coating is expected to form conducting network between particles and results in a superior discharge/charge performance.

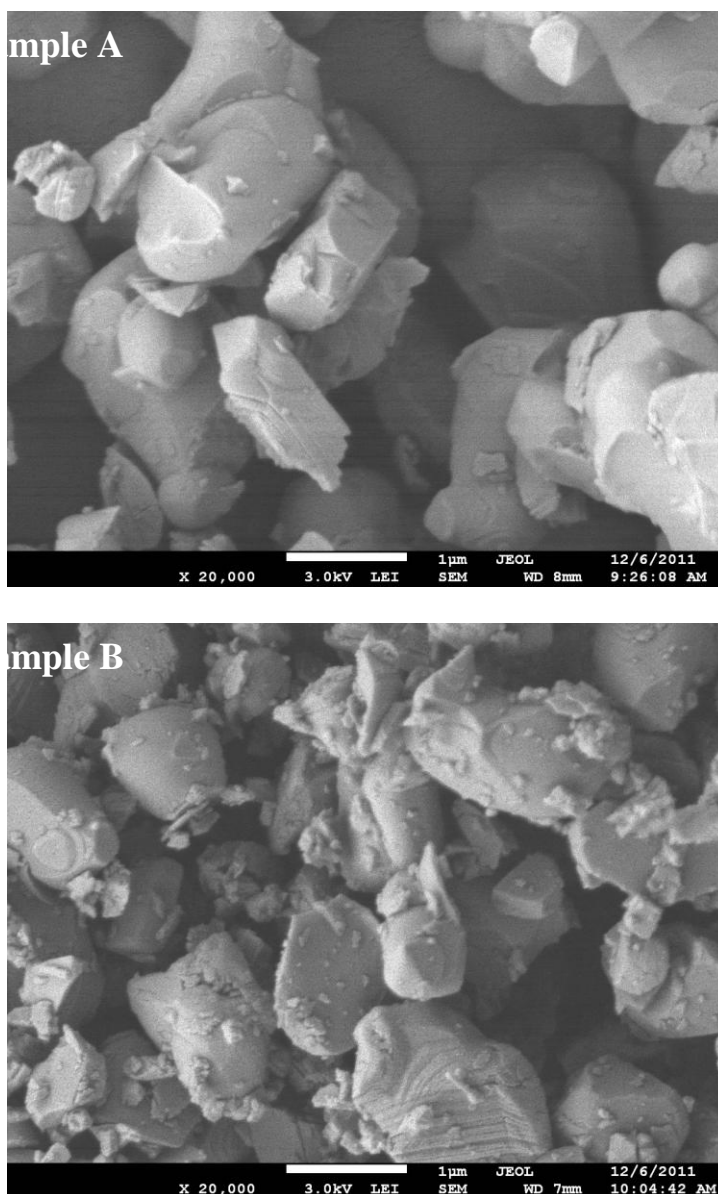


Figure 2. SEM images of (a) Sample A and (b) Sample B.

3.2 Electrochemical Performances

Fig. 3 presents the discharge capacities vs. cycle number of the pristine and $(\text{Li}_4\text{Ti}_5\text{O}_{12})_{100}/(\text{ZnO})_6$ anodes at 0.5, 1, 2, 3 and 4C rate ($1\text{C} = 170 \text{ mAhg}^{-1}$) in a potential range from 1.0 to 3.0 V at 20°C . With the surface modification of ZnO nanoparticles, $(\text{Li}_4\text{Ti}_5\text{O}_{12})_{100}/(\text{ZnO})_6$ (0.5C: 156 mAhg^{-1} ; 1C: 140 mAhg^{-1} ; 2C: 119 mAhg^{-1} ; 3C: 103 mAhg^{-1} ; 4C: 90 mAhg^{-1} , respectively) demonstrates higher capacity than Sample A (0.5C: 145 mAhg^{-1} ; 1C: 109 mAhg^{-1} ; 2C: 73 mAhg^{-1} ; 3C: 45 mAhg^{-1} ; 4C: 36 mAhg^{-1} , respectively), especially at high rate. The poor electron transfer activity among $\text{Li}_4\text{Ti}_5\text{O}_{12}$ particles is considered to be responsible for the inferior electrochemical performance of $\text{Li}_4\text{Ti}_5\text{O}_{12}$. The increment in discharge capacity suggests that the surface modification with ZnO would facilitate the electrochemical insertion/extraction process of Li^+ ion, especially at high rate.

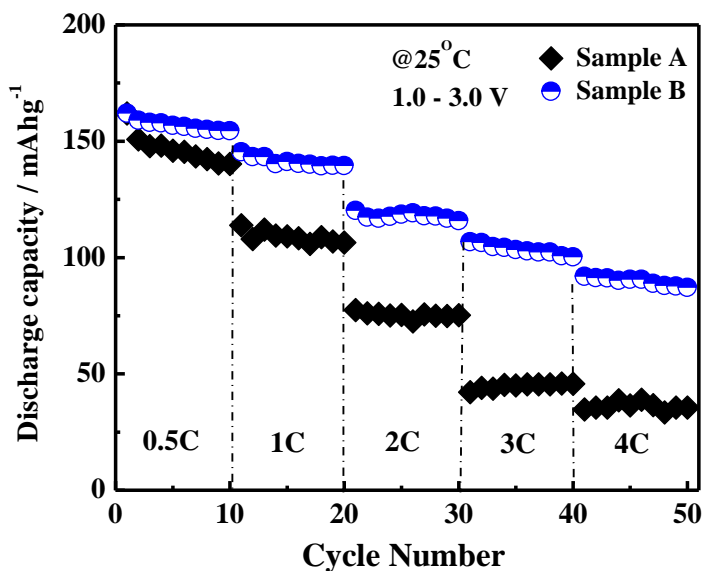


Figure 3. Rate capabilities of Samples A and B in a potential range from 1.0 to 3.0 V at 20 °C.

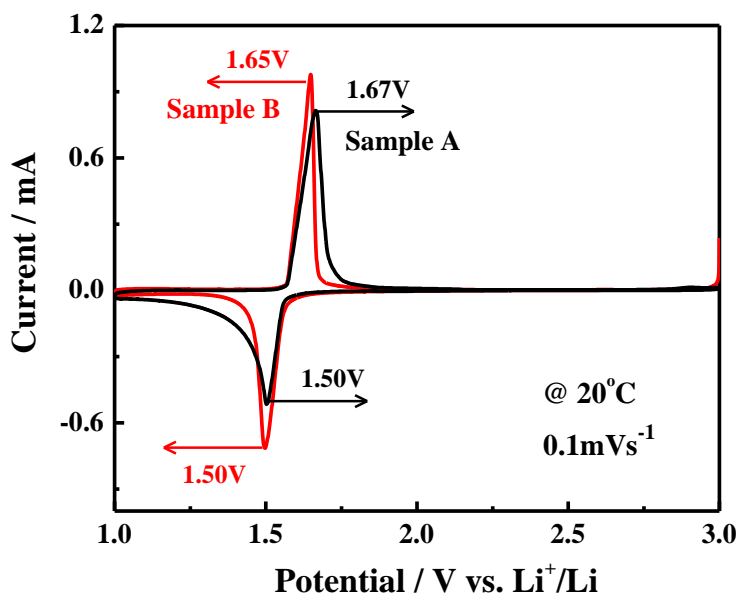


Figure 4. Cyclic voltammograms of Sample A and B between 1.0 and 3.0V at a scan rate of 0.1mVs⁻¹ at 20°C.

Cyclic voltammograms of Samples A and B at a scan rate of 0.1mVs⁻¹ between 1.0 and 3.0V are shown in Fig. 4. A pair of anodic and cathodic peaks occurs at around 1.55V versus Li⁺/Li, corresponding to the typical characteristic of electrochemical lithium insertion/extraction of Li₄Ti₅O₁₂ [14]. It is clear that both investigated electrodes have similar redox peaks, indicating that ZnO-incorporation does not change the electrochemical reaction process of Li₄Ti₅O₁₂. However, CV profile of Sample B exhibits more symmetric and sharper shape of the oxidation-reduction peaks than that of Sample A. In addition, The potential difference between anodic and cathodic peaks for Sample B (

$\Delta V=150\text{mV}$) has lower potential difference than the pristine $\text{Li}_4\text{Ti}_5\text{O}_{12}$ ($\Delta V=170\text{mV}$), suggesting that the incorporation of high electronic-conductive ZnO is favorable for reducing the electrode polarization.

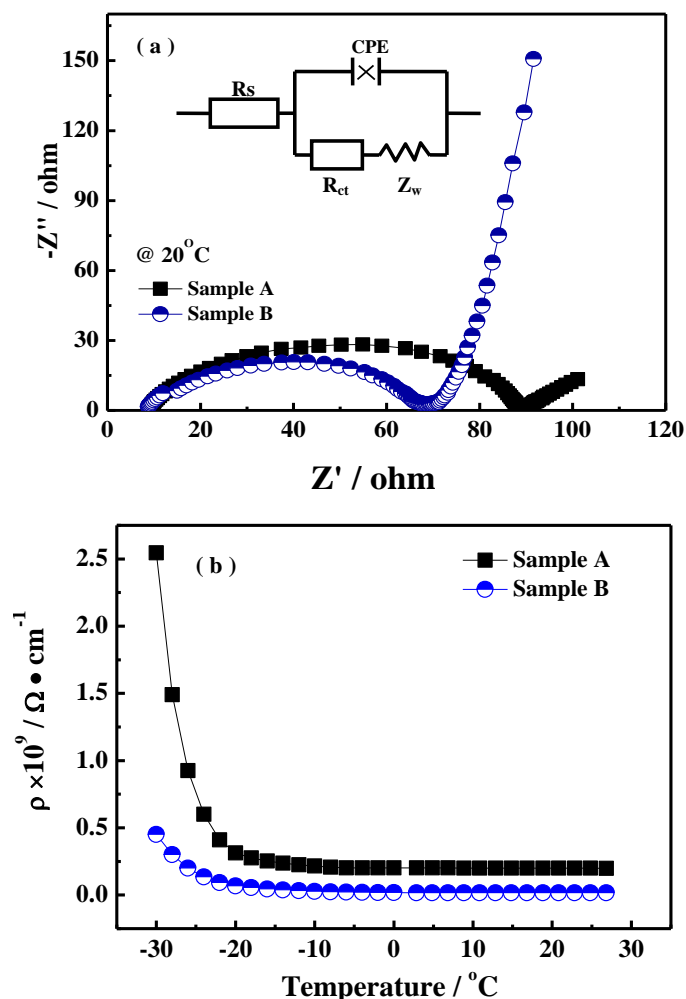


Figure 5. (a) EIS profiles of Samples A and B after 50 cycles at the stable voltage of 1.55 V at 20 °C. Inset is the equivalent circuit used for fitting the experimental impedance data; (b) The temperature dependence of the electrical resistivities of Samples A and B.

Fig.5(a) shows EIS impedance spectra of Samples A and B electrodes after 50 cycles, which are measured at the stable voltage of 1.55 V. EIS impedance spectra are fitted with the help of a modified Randle-Ershler equivalent circuit [15] (shown in the inset in Fig.5), where R_s and R_{ct} are the solution resistance and charge transfer resistance, respectively. CPE is placed to represent the double-layer capacitance and passivation-film capacitance, and Z_w is the Warburg impedance [16]. The fitted results reveal that Sample B electrode has smaller charge transfer resistance ($R_{ct}=56.09\Omega$) than that ($R_{ct}=73.56\Omega$) of Sample A. This might be due to the fact that $(\text{Li}_4\text{Ti}_5\text{O}_{12})_{100}/(\text{ZnO})_6$ has higher electronic-conductivity than the pristine $\text{Li}_4\text{Ti}_5\text{O}_{12}$ with the presence of ZnO. Fig.5(b) presents the temperature dependence of the electrical resistivity of Samples A and B, measured by a standard four-probe method from $-30\text{ }^\circ\text{C}$ to $27\text{ }^\circ\text{C}$. Both the testing sheets were made by pressing as-prepared powder under 20 MPa. It is found that Sample B has much smaller resistivity than Sample A in the whole

operation temperature range, resulting in facilitating the electron transport in the electrochemical lithium insertion/extraction process.

To investigate the effect of ZnO on the reversibility of Li^+ intercalation kinetics for $\text{Li}_4\text{Ti}_5\text{O}_{12}$, the electrochemical performances a potential range from 0.01 to 3 V are investigated. Fig.6 shows the cyclic performance of Sample A and B at 0.5, 1, 2, 3 and 4C rate at 20°C. In comparison with the pristine $\text{Li}_4\text{Ti}_5\text{O}_{12}$, Sample B demonstrates higher capacity and superior rate performance, especially at high charging/discharging rate. The larger initial discharge capacity of $(\text{Li}_4\text{Ti}_5\text{O}_{12})_{100}/(\text{ZnO})_6$ over theoretical capacity (298mAh^{-1}) of $\text{Li}_4\text{Ti}_5\text{O}_{12}$ might result from the lithiation in ZnO at low potential range [17].

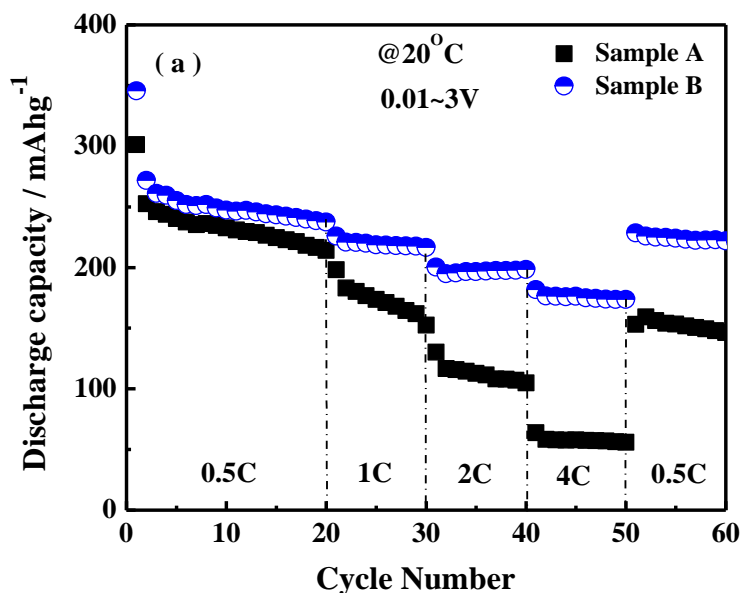


Figure 6. Rate capabilities of Samples A and B in a potential range from 0.01 to 3.0 V at 20 °C.

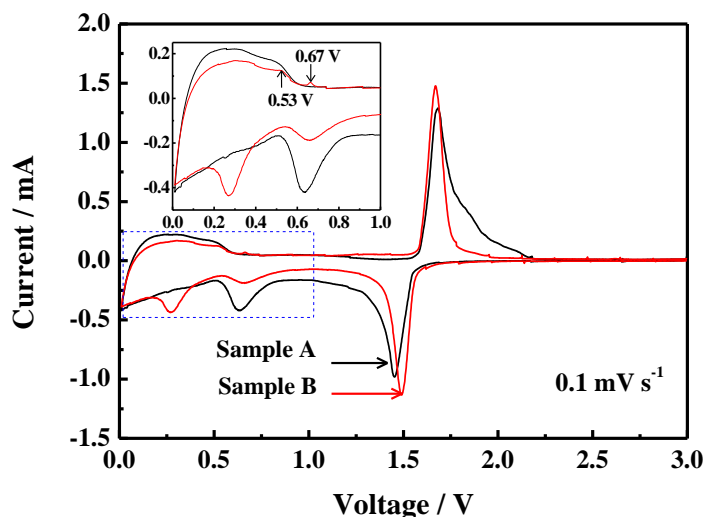


Figure 7. Cyclic voltammograms of Sample A and B between 0.01 and 3.0V at a scan rate of 0.1mVs^{-1} at 20 °C; Inset is an enlarged image of the CV in a potential range from 0.01 to 1.0 V.

Fig. 7 presents cyclic voltammograms of both samples with coin cell at a scan rate of 0.1 mVs^{-1} . The figure clearly shows that there are two pairs of redox peaks for each sample between 0.01 and 3V, suggesting that ZnO-incorporation does not change the electrochemical reaction process of $\text{Li}_4\text{Ti}_5\text{O}_{12}$. In comparison with $\text{Li}_4\text{Ti}_5\text{O}_{12}$, the peaks at low potential (0.53V, 0.67V) of $(\text{Li}_4\text{Ti}_5\text{O}_{12})_{100}/(\text{ZnO})_6$, shown in the inset, further confirms the contribution of ZnO in the discharge capacity of $(\text{Li}_4\text{Ti}_5\text{O}_{12})_{100}/(\text{ZnO})_6$ composite when cycled between 0.01 and 3.0 V [17,18].

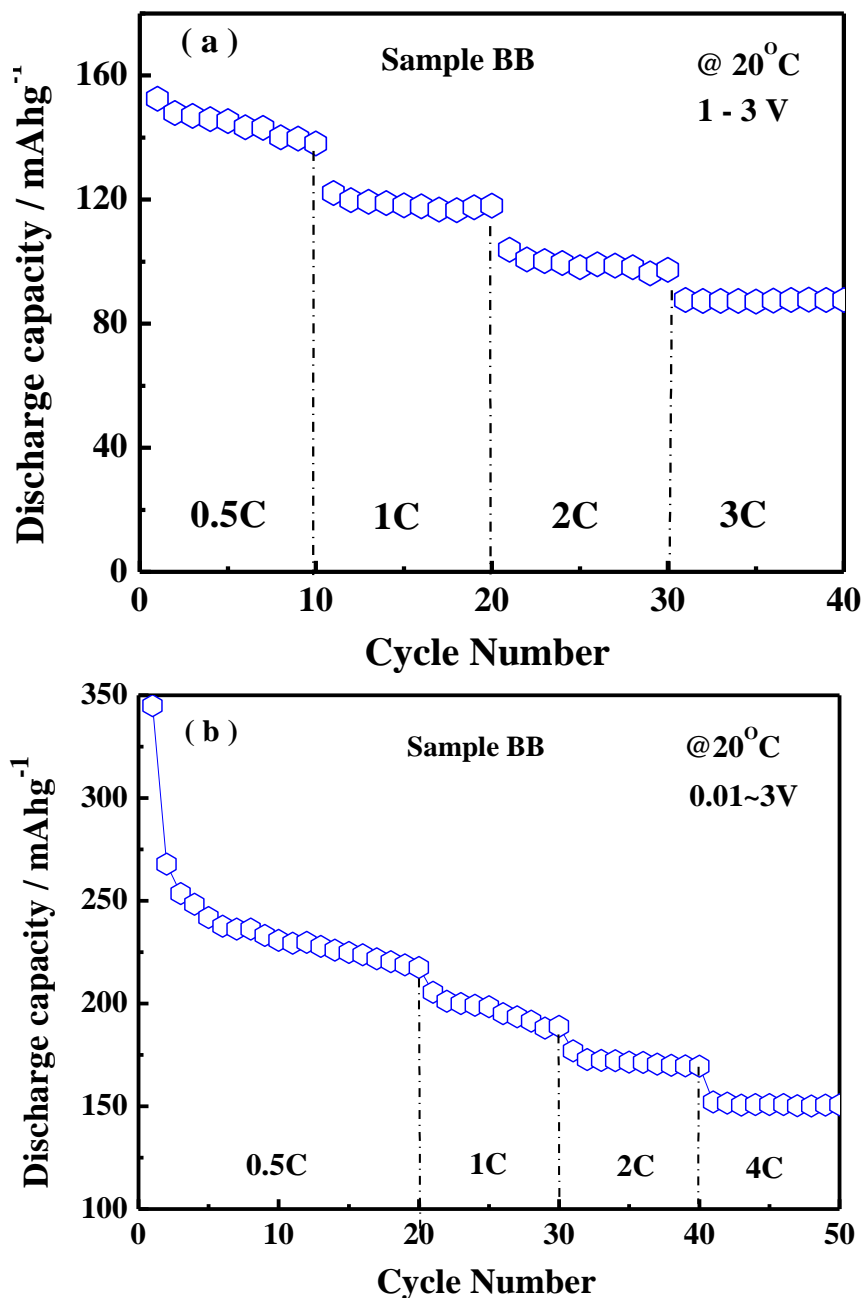


Figure 8. Rate capabilities of Samples BB in a potential range from (a) 1.0 to 3.0 V and (b) 0.01 to 3.0 V.

To get insight into the reason behind the enhancement of electrochemical performance with ZnO-incorporation, ZnO nanoparticles are calcined at $500 \text{ }^\circ\text{C}$ for 7 h in oxygen atmosphere and the

corresponding $(\text{Li}_4\text{Ti}_5\text{O}_{12})_{100}/(\text{ZnO})_6$ is correspondingly prepared, denoted as Sample BB. Figs. 8 (a) and (b) illustrate the discharge capacities of Sample BB at different discharge rates in a potential range from 1 to 3 V and 0.01 to 3 V, respectively. It is found that the specific capacities of Sample BB are superior to that of Sample A but inferior to that of Sample B in both cases, especially at high discharge current density. It is well-established that the electronic conductivity of ZnO is strongly dependent on the native point defects in ZnO, such as oxygen vacancies [19, 20]. The defects are assumedly reduced with thermal-treatment in oxygen atmosphere, leading to increase the resistivity of ZnO in composite. As a result, Sample BB with less oxygen vacancies in ZnO shows inferior rate capability in comparison with Sample B.

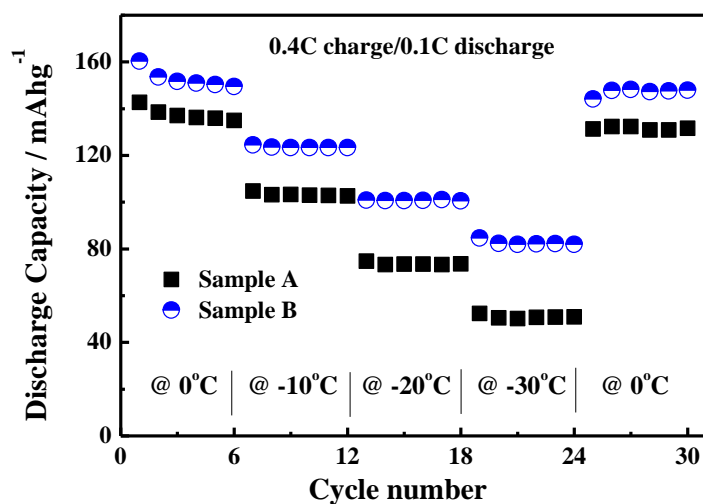


Figure 9. Cycling capabilities of Sample A and B at different temperature in a potential range from 1 to 3 V.

Excellent low-temperature performance of Li-ion battery is highly desired for specific applications [21]. Fig. 9 shows the rate capabilities of Samples A and B at various temperatures under 0.4C charge/0.1C discharge rate in a potential range from 1.0 to 3.0 V. Both electrodes exhibit relatively stable cycling stability resulting from the near zero volume variation during the charge/discharge process. In comparison, $(\text{Li}_4\text{Ti}_5\text{O}_{12})_{100}/(\text{ZnO})_6$ (0 °C: 160.3 mAhg⁻¹; -10 °C: 124.5 mAhg⁻¹; -20 °C: 100.9 mAhg⁻¹; -30 °C: 84.7 mAhg⁻¹, respectively) shows better electrochemical performance than that of $\text{Li}_4\text{Ti}_5\text{O}_{12}$ (0 °C: 142.7 mAhg⁻¹; -10 °C: 104.7 mAhg⁻¹; -20 °C: 74.7 mAhg⁻¹; -30 °C: 52.4 mAhg⁻¹, respectively). Analysis from the temperature dependence of the electrical resistivity reveals $(\text{Li}_4\text{Ti}_5\text{O}_{12})_{100}/(\text{ZnO})_6$ has much smaller resistivity than $\text{Li}_4\text{Ti}_5\text{O}_{12}$ especially at lower temperature, which is responsible for the superior low-temperature performance of Sample B.

To further investigate the mechanism of improved low-temperature performance with ZnO surface modification, the electrochemical impedance spectra (EIS) for Samples A and B were measured at the discharged state from 0 °C to -30 °C, as shown in Fig.10. All EIS diagrams are composed of a depressed semicircle at high frequencies and a spike at low frequencies. It is clear that the charge transfer resistance (R_{ct}) of Samples A and B increases rapidly with the temperature falling, which is

due to much more prominent resistance on the charge transfer reaction occurring at the electrode/electrolyte interface [21].

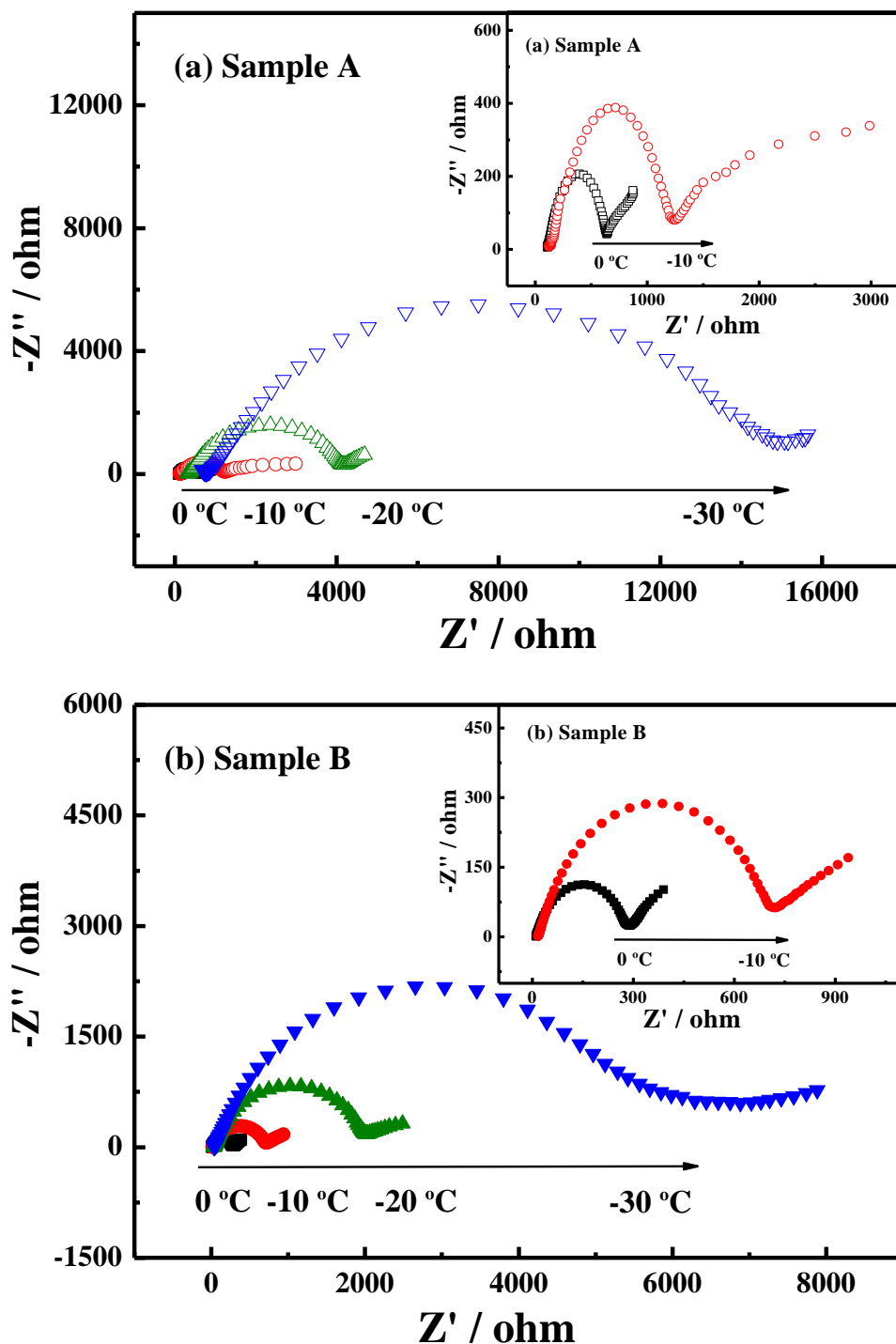


Figure 10. EIS for (a) Sample A and (b) Sample B at the stable voltage of 1.55 V in different operation temperatures.

Moreover the R_{ct} values of Sample B are all smaller than those of Sample A at various low temperatures, indicating higher conductivity of the composite [22] and better battery reaction kinetic than those of pristine $Li_4Ti_5O_{12}$. The increase of R_{ct} should be responsible for obvious capacity and

energy loss at low temperature, which is strongly dependent on the activation energy (ΔG) of electrode reaction. The activation energy (ΔG) can be calculated to characterize temperature (T) dependence of R_{ct} quantitatively by the following equation [23]:

$$\log R_{ct} = \log A + \frac{\Delta G - R}{2.303RT} \quad (1)$$

where R is the gas constant and A is a temperature-independent constant, respectively.

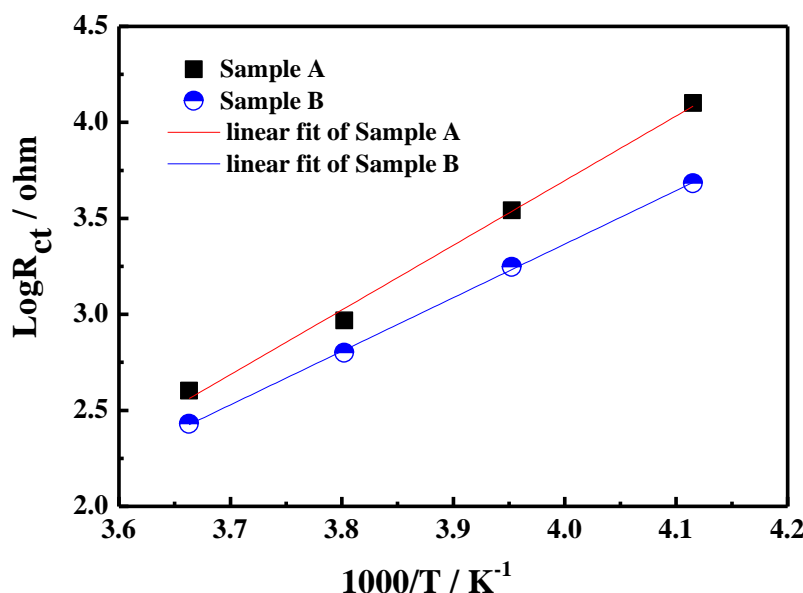


Figure 11. Profile of $\log(R_{ct})$ vs. temperature for Sample A and B.

The linear relationship between $\log R_{ct}$ and T^{-1} for both samples is well revealed in Fig.11. The calculated results mean that Sample B has lower values of ΔG (61.73 kJmol^{-1}) than that (72.84 kJmol^{-1}) of Sample A. The higher the value of ΔG is, the more the demanded energy for the intercalation/deintercalation of lithium-ion is. As a result, the surface reaction kinetics and electric conductivity of $\text{Li}_4\text{Ti}_5\text{O}_{12}$ at low-temperature could be improved by the surface modification of high electronic conductivity ZnO.

4. CONCLUSIONS

$\text{Li}_4\text{Ti}_5\text{O}_{12}$ incorporated with high electronic-conductive ZnO is synthesized by a simple mechanical method. Compared to $\text{Li}_4\text{Ti}_5\text{O}_{12}$, $(\text{Li}_4\text{Ti}_5\text{O}_{12})_{100}/(\text{ZnO})_6$ has superior rate and low-temperature performances. Analysis from electrical and PL properties indicate that the oxygen-vacancy-enriched ZnO nanoparticle on $\text{Li}_4\text{Ti}_5\text{O}_{12}$ should be an effective way on improving the electrode reaction kinetics and low-temperature electrochemical performances.

ACKNOWLEDGEMENTS

This work was supported by a grant from National Science Foundation for Young Scholars (No. 11004032) and Natural Science Foundation of China (No.11074039).

References

1. J. Jeong, Y. U. Kim, H. Kim, Y. J. Kim, H. J. Sohn, *Energy Environ. Sci.*, 4 (2011) 1986.
2. B. Scrosati, J. Garche, *J. Power Sources*, 195 (2010) 2419.
3. I. Belharouak, G. M. Koenig Jr., K. Amine, *J. Power Sources*, 196 (2011) 10344.
4. T. F. Yi, L. J. Jiang, J. Shu, C. B. Yue, R. S. Zhu, H. B. Qiao, *J. Phys. Chem. Solids* 71 (2010) 1236.
5. A. S. Aricò, P. Bruce, B. Scrosati, J. M. Tarascon, W. van Schalkwijk, *Nat. Mater.* 4 (2005) 366.
6. G. N. Zhu, Y. G. Wang, Y. Y. Xia, *Energy Environ. Sci.*, 5 (2012) 6652.
7. S. Scharner, W. Weppner, P. Schmid-Beurmann, *J. Electrochem. Soc.* 146 (1999) 857.
8. C. H. Chen, J. T. Vaughey, A. N. Jansen, D. W. Dees, A. J. Kahaian, T. Goacher, M. M. Thackeray, *J. Electrochem. Soc.* 148 (2001) A102.
9. X. F. Guo, C. Y. Wang, M. M. Chen, J. Z. Wang, J. M. Zheng, *J. Power Sources* 214 (2012) 107.
10. Z. M. Liu, N. Q. Zhang, Z. J. Wang, K. N. Sun, *J. Power Sources* 205 (2012) 479.
11. H. S. Li, L. F. Shen, X. G. Zhang, J. Wang, P. Nie, Q. Chen, B. Ding, *J. Power Sources* 221 (2013) 122.
12. H. B. Wang, Q. M. Pan, Y. X. Cheng, J. W. Zhao, G. P. Yin, *Electrochem. Acta.* 54 (2009) 2851.
13. J. P. Liu, Y. Y. Li, R. M. Ding, J. Jiang, Y. Y. Hu, X. X. Ji, Q. B. Chi, Z. H. Zhu, X. T. Huang, *J. Phys. Chem. C* 113 (2009) 5336.
14. J. Q. Deng, Z. G. Lu, I. Belharouak, K. Amine, C. Y. Chung, *J. Power Sources* 193 (2009) 816.
15. K. Dokko, M. Mohamedi, M. Umeda, I. Uchida, *J. Electrochem. Soc.* 150 (2003) A425.
16. D. Yoshikawa, Y. Kadoma, J. M. Kim, K. Ui, N. Kumagai, N. Kitamura, Y. Idemoto, *Electrochim. Acta*, 55 (2010) 1872.
17. X. H. Huang, X. H. Xia, Y. F. Yuan, F. Zhou, *Electrochem. Acta.* 56 (2011) 4960.
18. H. Q. Dai, H. Xu, Y. N. Zhou, F. Lu, Z. W. Fu, *J. Phys. Chem C*, 116 (2012) 1519.
19. Ü. Özgür, Ya. I. Alivov, C. Liu, A. Teke, M. A. Reshchikov, S. Doğan, V. Avrutin, S.-J. Cho, and H. Morkoç, *J. Appl. Phys.* 98 (2005) 041301.
20. C. F. Yu, C. W. Sung, S. H. Chen, S. J. Sun, *Appl. Surf. Sci.* 256 (2009) 792.
21. T. Yuan, X. Yu, R. Cai, Y. k. Zhou, Z..p. Shao, *J. Power Sources.* 195 (2010) 4997.
22. S. H. Huang, Z. Y. Wen, B. Lin, J. D. Han, X. G. Xu, *J. Alloys Compds.* 457 (2008) 401.
23. J. Li, C. F. Yuan, Z. H. Guo, Z. A. Zhang, Y. Q. Lai, J. Liu, *Electrochim. Acta*, 59 (2012) 69.